AD-A185 393 A FUNDAMENTAL STUDY OF P/M PROCESSED ELEVATED TEMPERATURE ALUMINUM ALLOYS..(U) DREXEL UNIV PHILADELPHIA PA DEPT OF MATERIALS ENGINEERING 1/1

UNCLASSIFIED A LAWLEY ET AL. JUL 87 AFOSR-TR-87-0964 F/G 11/6.1 NL

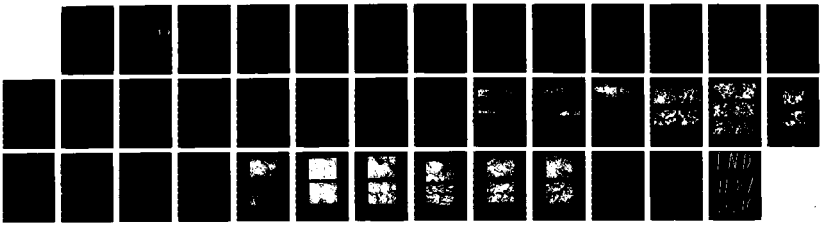

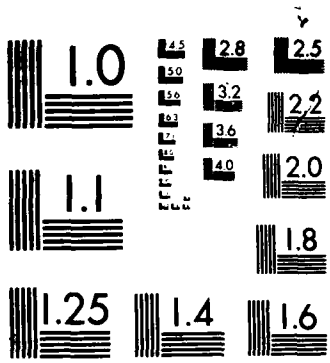


MICROCOPY RESOLUTION TEST CHART
NATIONAL BUREAU OF STANDARDS-1963-A

AD-A185 393

DTIC FILE COPY

AFOSR-TR- 87-0964

FINAL REPORT

# "A FUNDAMENTAL STUDY OF P/M PROCESSED ELEVATED TEMPERATURE ALUMINUM ALLOYS"

DTIC
ELECTE
SEP 3 0 1987
S D
D

AFOSR Grant #82-0010

Principal Investigators: A. Lawley and M.J. Koczak

Department of Materials Engineering

Drexel University

Philadelphia, PA 19104

DISTRIBUTION STATEMENT A
Approved for public release;
Distribution Unlimited

July 1987

87 9 24 061

Unclassified

SECURITY CLASSIFICATION OF THIS PAGE (When Data Entered)

# REPORT DOCUMENTATION PAGE

READ INSTRUCTIONS BEFORE COMPLETING FORM

1. REPORT NUMBER: AFOSR-TR- 87-0964

2. GOVT ACCESSION NO.

3. RECIPIENT'S CATALOG NUMBER

4. TITLE (and Subtitle)

A FUNDAMENTAL STUDY OF P/M PROCESSED ELEVATED TEMPERATURE ALUMINUM ALLOYS

5. TYPE OF REPORT & PERIOD COVERED

FINAL REPORT
10/1/81 - 9/30/86

6. PERFORMING ORG. REPORT NUMBER

7. AUTHOR(s)

A. Lawley and M.J. Koczak

8. CONTRACT OR GRANT NUMBER(s)

AFOSR-82-0010

9. PERFORMING ORGANIZATION NAME AND ADDRESS

Department of Materials Engineering
Drexel University
Philadelphia, PA 19104

10. PROGRAM ELEMENT, PROJECT, TASK AREA & WORK UNIT NUMBERS

61102F
2306/A1

11. CONTROLLING OFFICE NAME AND ADDRESS

Air Force Office ofScientific Research
Bolling AFB, Building 410
Washington, D.C. 20332

NE

12. REPORT DATE

July 1987

13. NUMBER OF PAGES

37

14. MONITORING AGENCY NAME & ADDRESS(if different from Controlling Office)

Scimo Co 11

15. SECURITY CLASS. (of this report)

Unclassified

15a. DECLASSIFICATION DOWNGRADING SCHEDULE

16. DISTRIBUTION STATEMENT (of this Report)

Approved for public release; distribution unlimited.

17. DISTRIBUTION STATEMENT (of the abstract entered in Block 20, if different from Report)

18. SUPPLEMENTARY NOTES

19. KEY WORDS (Continue on reverse side if necessary and identify by block number)

Aluminum-iron-cerium alloys; powder metallurgy; rapid solidification; mechanical alloying; microstructure; microstructural stability; elevated temperature tensile and creep properties; dispersion strengthening.

20. ABSTRACT (Continue on reverse side if necessary and identify by block number)

Ambient and elevated temperature tensile and creep response, and microstructural stability of a powder processed Al-Fe-Ce alloy have been evaluated. Gas atomized Al-Fe-C was mechanically alloyed (MA) to give a volume fraction of dispersoids of about 0.23. The powder was cold isostatically pressed in aluminum cans, outgassed and hot extruded to full density.

.....Continued

DD FORM 1 JAN 73 1473

Unclassified

SECURITY CLASSIFICATION OF THIS PAGE (When Data Entered)

Consistent with improved microstructural stability at elevated temperatures, the MA material is stronger and more creep resistant than the non-MA material. These improvements are attributed to the presence of fine scale oxides and carbides distributed uniformly throughout the structure, and which are introduced during MA; the dispersion inhibits coarsening. recpvery and recrystallization. Non-MA Al-Fe-Ce is stronger than non-MA Al-Fe-Ni at all temperatures but it has limited ductility. Qualitatively, the effect of MA on Al-Fe-Ce is similar to that in Al-Fe-Ni. These results suggest that Ce alters the transformation characteristics of Al-Fe and/or that Ce diffuses more slowly than Ni in Al, in the presence of Fe.

TABLE OF CONTENTS


ABSTRACT OF RESULTS i

INTRODUCTION 1

THE PRESENT PROGRAM 2

EXPERIMENTAL PROCEDURES 3

- Materials and Processing 3
- Microstructural Characterization 3
- Mechanical Testing 4

RESULTS AND OBSERVATIONS 5

- Microstructure 5
- Hardness and Tensile Properties 6
- Creep Response 7
- Fracture Behavior 7

INTERPRETATION AND SIGNIFICANCE OF RESULTS 8

- Microstructural Stability 8
- Creep Response 9
- Comparison of Al-Fe-Ce and Al-Fe-Ni 9

REFERENCES 11

TABLES AND FIGURES

PUBLICATIONS AND DISSERTATIONS

FORM DD 1473



DTIC COPY INSPECTED 2

Accession For
NTIS GRA&I
DTIC TAB
Unannounced
Justification
By
Distribution
Availability Codes
Dist
A-1

## ABSTRACT OF RESULTS

## ELEVATED TEMPERATURE DISPERSION STRENGTHENED ALUMINUM ALLOYS

- Powder Processed Rapidly Solidified and Mechanically Alloyed Al-Fe-Ce

Ambient and elevated temperature tensile and creep response, and microstructural stability of a powder processed Al-Fe-Ce alloy have been evaluated. Gas atomized Al-Fe-C was mechanically alloyed (MA) to give a volume fraction of dispersoids of about 0.23. The powder was cold isostatically pressed in aluminum cans, outgassed and hot extruded to full density.

Consistent with improved microstructural stability at elevated temperatures, the MA material is stronger and more creep resistant than the non-MA material. These improvements are attributed to the presence of fine scale oxides and carbides distributed uniformly throughout the structure, and which are introduced during MA; the dispersion inhibits coarsening, recovery and recrystallization. Non-MA Al-Fe-Ce is stronger than non-MA Al-Fe-Ni at all temperatures but it has limited ductility. Qualitatively, the effect of MA on Al-Fe-Ce is similar to that in Al-Fe-Ni. These results suggest that Ce alters the transformation characteristics of Al-Fe and/or that Ce diffuses more slowly than Ni in Al, in the presence of Fe.

- Powder Processed Rapidly Solidified and Mechanically Alloyed Al-Fe-Ni

The ambient and elevated temperature tensile and creep response, and microstructural stability of a powder processed Al-Fe-Ni alloy has been evaluated. Air atomized Al-Fe-Ni was blended with aluminum powder and mechanically alloyed (MA) to give a 0.19 volume fraction of $FeNiAl_9$ dispersoid (~0.18 μm); the powder was cold isostatically pressed in aluminum cans, outgassed, sealed and hot extruded to full density.

The MA alloy is stronger than the non-MA alloy at temperatures up to about 300°C. In addition, MA enhances microstructural stability at elevated temperature; for example there is no significant coarsening of the $FeNiAl_9$ after 624 hours at 450°C. Similarly, there is a significant enhancement in creep resistance over the range 250-350°C, compared to the same alloy without MA. Improvements in alloy strength and creep resistance are attributed to the presence of fine-scale (~30nm) oxides and carbides introduced during MA, and which are distributed uniformly throughout the matrix, at matrix-intermetallic interfaces, and on subgrain boundaries. This fine-scale dispersoid provides effective resistance to dislocation bowing (Orowan mechanism) below about 300°C. At higher temperatures, the fine scale dispersion inhibits coarsening and appears to interact with the diffusing Fe and Ni atoms. Microstructural stability is a function of the powder processing temperatures for degassing and extrusion.

- Powder Processed Rapidly Solidified Al-Fe-Ni

The elevated temperature tensile and creep response of powder metallurgy Al-Fe-Ni alloys with $FeNiAl_9$ dispersoid volume fractions of 0.19, 0.25 and 0.32 have been determined. The air atomized powders were consolidated to full density by vacuum hot pressing and/or hot extrusion. Powder and consolidate were characterized by means of optical and transmission electron microscopy, scanning electron microscopy, x-ray diffraction and differential scanning calorimetry. Tensile and creep tests were conducted at temperatures up to 400°C.

As atomized powders exhibit a duplex microstructure consisting of coarse and fine regions of $FeNiAl_9$ in the aluminum matrix. These microstructures are understood

in terms of the extent of droplet undercooling and the subsequent solidification velocities during atomization. The two scales of microstructure are retained after hot consolidation. The dispersoid is resistant to coarsening up to approximately 400°C. At higher temperatures, the measured coarsening rates are higher than those predicted by the LSW theory for volume diffusion, but are in agreement with a grain boundary diffusion model. Ambient temperature strengthening can be explained by the Orowan dislocation bowing model. Yield strength decreases with increasing temperature and above 300°C, it is independent of dispersoid size and dispersoid volume fraction. Steady state creep rate is independent of the dispersoid size and dispersoid volume fraction over the temperature range 250°C - 400°C, and the average stress exponent is 10 with a creep activation energy of 76 Kcal.mole. Elevated temperature deformation is consistent with a cooperative dislocation climb mechanism which is insensitive to dispersoid size and dispersoid volume fraction.

## INTRODUCTION

For many years, high strength aluminum alloys have served as the primary structural material in advanced military aircraft. These alloys are easy to fabricate, relatively inexpensive, and exhibit a high strength to weight ratio. Conventional ingot metallurgy aluminum alloys do, however, undergo significant decreases in strength and stiffness with increasing temperature, and this has acted as a major design constraint in limiting aircraft speeds to the Mach 2 Level. Based on existing materials technology, aircraft operation at higher speeds mandates the use of titanium alloys for many structural components with an accompanying penalty in terms of cost and weight. Thus, the need exists for the development of a new series of high performance aluminum alloys, with improved properties and elevated temperature stability. The initial goal of the U.S. Air Force is to develop aluminum-base alloys for long-time service in the temperature range 230-350°C.

There are several inherent limitations to achieving property and performance goals via ingot metallurgy (I/M) and this has stimulated research into powder metallurgy (P/M) as a processing alternative (1,2). Of particular interest is the technology of rapid solidification processing of aluminum alloys, since it has been demonstrated that this approach provides enhanced alloying flexibility, and results in refined fine-scale homegeneous microstructures with minimal attendent solute segregation, compared to I/M alloys (3-6).

To date several binary and ternary aluminum alloys have been investigated (3,5,6,7-11). The selection of the second and third alloying elements has been based primarily on the following criteria: high liquid solubility in aluminum, a low solid solubility in aluminum, and a low rate of solid state diffusion in aluminum. The first criterion permits large alloying additions to be made to the melt, while the second criterion ensures almost complete precipitation on cooling to form a high volume fraction of second phase particles (e.g. intermetallics). If the particles are strong and non-deformable, dislocations will be forced to bow between them during deformation. For a given particle size, an increase in the volume fraction of the second phase

particles decreases inter-particle spacing, which in turn increases strength. Further, if the intermetallic particles have high elastic moduli, then a material containing a high volume fraction of such particles will have a high Young's modulus.

The upper temperature limit is set by the stability or resistance to coarsening of the dispersed particles. Hence, it is necessary that the alloying elements selected have low rates of diffusion in solid aluminum. This third criterion minimizes the rate of coarsening of the dispersed particles at elevated temperatures.

On the basis of these criteria, the alloying elements selected in the development of a new class of high temperature aluminum alloys are the transition elements Cr, Mn, Fe, Ni and Co, and the rare earth element Ce. Alloy systems that show distinct promise in achieving property and performance goals at elevated temperature are Al-Fe-Ni, Al-Fe-Ce and Al-Fe-Mo, (12). The fine-scale intermetallic dispersoid, uniformly distributed throughout the aluminum matrix, is achieved by atomization of the molten alloy with its intrinsic component of rapid solidification. Subsequently the powder is hot consolidated to full density.

In this report, emphasis is placed on work completed in the final year of the program on Al-Fe-Ce. The high temperature tensile and creep properties, and microstructural stability were assessed with and without mechanical alloying as a processing step after atomization but prior to consolidation. Comparisons are also made with the elevated temperature behavior of Al-Fe-Ni which was previously studied extensively in this program.

## THE PRESENT PROGRAM

In the first phase of this program, optimum P/M processing conditions in the Al-Fe-Ni system were established with respect to microstructure and mechanical properties (13-15). Three volume fractions of $FeNiAl_9$ dispersoids were examined, namely 0.19, 0.25 and 0.32. Ambient and elevated temperature tensile and creep response were assessed at temperatures up to 400°C and microstructural stability was evaluated at temperatures up to 500°C.

A fine scale uniform distribution of dispersoids can also be introduced into an alloy by mechanical alloying (MA), (16-21). In the second phase of this program we have examined the effect of MA on P/M processed Al-Fe-Ni with respect to strength and microstructural stability (22,23). The atomized alloy was subjected to a MA step prior to hot consolidation. A significant improvement in elevated temperature strength and creep resistance was observed, compared to the non-MA alloy. Furthermore, long-time microstructural stability was demonstrated up to about 450°C. MA results in a fine-scale dispersion of $Al_2O_3$ since the process breaks up oxide films present on powder particle surfaces, and it also introduces small dispersoids of $Al_4C$. The source of carbon is the process-control agent added to prevent excessive welding during MA.

In the final phase of this program the effect of MA on the microstructural stability and elevated temperature tensile and creep response of an Al-Fe-Ce alloy containing approximately 20 Vol % dispersed phase has been examined. Several recent studies on P/M processed Al-Fe-Ce without MA provide a base-line for comparison (7-10).

## EXPERIMENTAL PROCEDURES

### Materials and Processing

Al-Fe-Ce powder of nominal composition Al-8.07%Fe - 3.95%Ce by weight was gas atomized by Alcoa. A portion of the powder was mechanically alloyed (MA) at Novamet using Stearic acid as a process control agent. This prevented excessive welding of the powder to itself and to the steel balls.

Both MA and non-MA Al-Fe-Ce powders were cold isostatically pressed in aluminum cans, outgassed at 425°C and sealed. Finally, the sealed compacts were hot extruded to full density at 425°C using an extrusion ratio of 16:1 to give 12.7 mm dia rod. The hot extrusion was performed by Nuclear Metals, Inc.

### Microstructural Characterization

Consolidated MA and non-MA material was examined by optical microscopy (OM) and transmission electron microscopy (TEM) in the extruded condition, and after

elevated temperature exposure. Sample preparation for OM involved grinding, diamond polishing and etching, using Keller's reagent for about 10 seconds. TEM studies were conducted on a JEM 100CX II microscope at an accelerating voltage of 100KV. Sample preparation consisted of slicing with a diamond wheel to a section thickness of about 1mm. The sections were surface ground to a thickness ~ 0.004mm and discs stamped out for subsequent thinning via electrolytic jet polishing. The electrolyte consisted of 75% methanol and 25% nitric acid; it was kept at a temperature between -30 and -40°C. Considerable difficulty was experienced in electropolishing the MA material. Acceptable electron - transparent foils were obtained using an electrolyte of 80% ethanol (200 proof) and 20% perchloric acid, by volume, at about -40°C.

**Mechanical Testing**

Hardness (Rockwell B. scale) was determined at ambient temperature in the as extruded condition, and following elevated temperature exposure. These exposures were isochronal (1 hour up to 550°C) or isothermal (up to 300 hours at 450°C).

Tensile tests were performed on a Model 1127 Instron at temperatures up to 400°C (±2°C). Threaded end specimens were used with a 32mm gage length and a 6.35mm gage diameter. The tensile load was applied parallel to the extrusion direction. Tests were carried out to fracture in air at a strain rate of $2.65 \times 10^{-4}$ $sec^{-1}$.

Creep tests were performed in air under a constant tensile load in a SATEC lever arm test machine. The size, geometry, and orientation of the creep specimens were identical to those of the tensile specimens. Creep strain was monitored with a linear variable differential transformer that measured the displacement of the grip linkage outside the furnace. Rupture life was determined as a function of stress and temperature. Creep tests resulting in very small strain rates were terminated at times under 150 hours without failure of the sample.

Fracture surfaces of the tensile and creep specimens were examined directly via scanning electron microscopy (SEM) in a JSM 35CF microscope.

## RESULTS AND OBSERVATIONS

### Microstructure

Representative optical micrographs of the non-MA and MA Al-Fe-Ce in the as-extruded condition are shown in Figure 1. Corresponding microstructures after elevated temperature exposure (420°C, 450°C and 603°C) are shown in Figure 2 (non- MA) and Figure 3 (MA). At this level of resolution there is no significant change in microstructure in the non-MA and MA material after a 1 hour expsoure at 420°C. Coarsening of the dispersoids occurs in both the non-MA and the MA materials at 450°C; most of the microstructural change has occurred after 8 hours. Significant coarsening is evident after a 1 hour exposure at 603°C; the effect is more pronounced in the non-MA material.

Further insight into the as-extruded microstructure and microstructural changes occurring at elevated temperatures is provided by TEM. Representative microstructures are shown in Figures 4(a) and 4(b) for as extruded non-MA and MA material respectively. MA introduces fine-scale dispersoids of oxides and carbides in the nanometer size range. In general, the microstructure is more homogeneous in the MA material. A range of dispersoid sizes and morphologies exists. Microstructures were also examined close to the fracture surface after tensile testing at ambient and elevated temperatures. The dispersoid structure appears to be insensitive to plastic deformation.

The effect of elevated temperature exposure is illustrated in Figures 5 and 6, for the non-MA and MA materials respectively. After a 1 hour exposure at 610°C, the dispersoids in the MA material are still relatively fine. Spherical dispersoids exist in two size ranges; a fine size range with an average diameter of about 0.05μm, and a coarser size range with an average diameter of about 0.3μm. Acicular particles range in length from 0.06μm to 0.5μm. After coarsening, the aspect ratio of these particles decreases; typically, this ratio is about 9 in the as-extruded condition and it decreases to about 3 after exposure at or above 450°C.

A characteristic feature of the coarsened microstructures is the appearance of a

very fine-scale precipitate distributed uniformly throughout the matrix, Figures 5 and 6. The subgrain size is about 0.25μm in the as-extruded condition; this increases to ~0.4μm and ~0.7μm after exposure at 450°C and 603°C, respectively.

## Hardness and Tensile Properties

Room temperature hardness for both non-MA and MA material after isothermal exposure at 450°C for times up to 288 hours is shown in Figure 7. In the as-extruded condition, the MA material is harder than the non-MA material by about $18R_B$ points. These data confirm the superiorty of the MA material compared to the non-MA material with respect to hardness retention, and hence elevated temperature microstructural stability. After 288 hours at 450°C, the hardness decreases in the MA and non-MA materials are about 8% and 68%, respectively. Consistent with the microstructural observations, most of the hardness decrease in the non-MA material occurs at short elevated temperature exposure times, Figure 7; beyond 50 hours, further decreases in hardness are smaller.

Hardness response, measured at room temperature, following isochronal (1 hour) elevated temperature exposure is shown in Figure 8. In the non-MA material hardness decreases slowly when the exposure temperature is below ~400°C; above this temperature there is a sharp drop in hardness. In comparison, the MA material retains its hardness at exposure temperatures up to 500°C, beyond which hardness drops significantly.

A comparison of the temperature dependence of tensile strength in the non-MA and MA materials is made in Figure 9. The MA material is stronger than the non-MA material at all temperatures. The rate of decrease in strength with temperature is similar in the non-MA and MA conditions. The increase in strength brought about by MA is accompanied by a drastic reduction in ductility at all temperatures, as measured by the tensile strain to failure, Figure 10. The extent of work hardening is reduced by MA, particularly in the lower temperature range. For this reason, strength data in

Figure 9 for the MA material refer to the fracture stress.

**Creep Response**

Creep curves for the non-MA material for several combinations of stress and temperature are illustrated in Figure 11. The tests at 250°C/103MPa and 350°C/83MPa were stopped after 100 hours without failure. Examples of creep curves for the MA material are shown in Figure 12.

Comparison of the creep response of non-MA and MA materials at the same conditions of stress and temperature is made in Figure 13. The corresponding steady state (minimum) creep rates are summarized in Table I; these data demonstrate the significant enhancement in creep resistance as a result of MA.

**Fracture Behavior**

Representative SEM microstructures of the MA and non-MA material adjacent to the fracture surfaces after tensile deformation at 400°C are illustrated in Figure 14. Failed specimens were sectioned parallel to the loading direction (ie. the extrusion axis); the areas shown in Figure 14 are located just beneath the fracture surface. In the non-MA samples, voids have opened transverse to the stress direction, Figure 14(a). No voids were observed in the MA material; this is attributed to the limited ductility of the alloy in this condition. The dark areas in Figure 14(b) are believed to be microstructural inhomogeneities such as regions devoid of dispersoids adjacent and parallel to regions containing microcracks.

Fracture surface morphologies following tensile deformation at ambient and 340°C are shown in Figures 15 and 16 for the non-MA and MA materials, respectively. The non-MA material fails by dimpled rupture at both temperatures. Elongation to failure is similar in the non-MA material at both temperatures. However, grain boundary cavitation is much more pronounced following deformation at 340°C than at ambient. Consistent with its limited ductility, cleavage is a characteristic feature of the MA fracture surface after deformation at room temperature, Figure 16(a). There is a small increase in ductility in the MA material at elevated temperatures (Figure 10), and there is a corresponding decrease in the area of cleavage on the fracture surfaces, Figure

16(b).

Representative creep fracture surface morphologies for the non-MA material are shown in Figures 17, 18 and 19. These fractographs show that the primary failure mode is microvoid coalescence. For the duration of the creep tests run on the MA material, the total creep strains were small (<0.35%) and the specimens did not rupture.

## INTERPRETATION AND SIGNIFICANCE OF RESULTS

### Microstructural Stability

From the TEM observations, it is clear that a spectrum of dispersoid sizes and morphologies exists. In an alloy of similar composition but without MA as a processing step, Angers et al. (10) have identified the dispersed particles as the equilibrium phases $Al_{13}Fe_4$ and $Al_{10}Fe_2Ce$. They are incoherent with the matrix and constitute 23% by volume of the alloy. Coarsening of both dispersoids was shown to occur primarily via the mechanisms of solute diffusion along dislocations and grain boundaries.

Primary dispersoid morphologies in the non-MA and MA material are equiaxed and acicular. Similar observations have been reported by Swanson and Kim (24) in melt spun Al-8%Fe-8%Ce and Al-8%Fe-4.5%Ce-0.7%W. The spherical particles were in the size range 0.20-0.1μm and acicular particles were about 0.02μm wide x 0.2μm long. Tip radius at the ends of the acicular particles was larger in the present study.

For the dispersoids to coarsen, diffusion of Fe and Ce atoms must occur, either via the subgrain boundaries or through the matrix. MA introduces a very fine scale, uniform dispersion of oxides and carbides. Those oxides and carbides on a subgrain boundary may be expected to inhibit diffusion along this path by acting as vacancy sinks. The dispersion may also attract Fe and Ce atoms diffusing through the lattice by forming oxides and/or carbides. Thus coarsening of the dispersoid becomes more and more difficult. This is the basis of the higher stability of the MA alloy, compared to the non-MA alloy.

Apart from resistance to coarsening, the fine dispersion of oxides and carbides in the MA material inhibits recrystallization because of the pinning of subgrain boundaries (20). In the non-MA material, the higher rate of dispersoid coarsening promotes recrystallization with an attendant release of subgrain boundaries and subsequent grain growth. After 288 hrs. at 450°C, the subgrain size in non-MA material is about 1μm, compared to a subgrain size of 0.25μm in the as-extruded condition.

## Creep Response

In terms of creep response, the MA material is significantly more resistant to strain than the non-MA alloy, under identical test conditions, Table I. In the MA material, submicron dispersoids enhance creep resistance by trapping dislocation clusters in cell walls thereby effectively impeding recovery, and also by acting as a barrier to diffusion mechanisms.

## Comparison of Al-Fe-Ce and Al-Fe-Ni

In the non-MA condition, the Al-Fe-Ce alloy is considerably stronger than the Al-Fe-Ni alloy at all temperatures (14,15). At ambient temperature the differential in tensile strength is about 26%, and this increases to about 69% at 400°C. The hardness profiles following elevated temperature exposure (Figures 7 and 8) for non-MA Al-Fe-Ce are noticeably higher than the corresponding plots for non-MA Al-Fe-Ni (13-15). Under the same conditions of stress and temperature, the creep resistance of non-MA Al-Fe-Ce is superior to that of non-MA Al-Fe-Ni. For example, at 350°C/83 MPa, Al-Fe-Ni failed in less than two hours, whereas the Al-Fe-Ce alloy exhibited negligible strain after 100 hours (14,15).

It has been suggested that the presence of Ce in Al-Fe alters the nucleation characteristics (25). The transformation is slower and the aspect ratio of the acicular phase in Al-Fe-Ce is different from that in Al-Fe. This may also explain the difference in mechanical behavior of non-MA Al-Fe-Ce and Al-Fe-Ni. The large difference in strength at 400°C reflects the superior microstructural stability of Al-Fe-Ce compared to

Al-Fe-Ni. The difference in creep response in the two systems is consistent with the hypothesis that the diffusivity of Ce in Al is slower than that of Ni in Al.

Qualitatively, the effect of MA on Al-Fe-Ce is similar to that in Al-Fe-Ni. Thus, microstructural stability above ambient and elevated temperature strength are enhanced in both systems as a result of MA. Hardness response in both systems after elevated temperature exposure under isothermal or isochronal conditions is comparable (13-15).

On the basis of the results and observations from this program, several follow-on approaches are suggested. Blending of the Al-Fe-Ce powder with pure Al powder prior to MA would reduce the volume fraction of dispersoids and may result in an increase in ductility. Differences in the mechanical behavior between non-MA and MA Al-Fe-Ce are similar to those in the Al-Fe-Ni system. The accompanying microstructural changes, however, are apparently more complicated in Al-Fe-Ce than Al-Fe-Ni and deserve further attention. DSC and DTA of the non-MA and MA Al-Fe-Ce should provide insight into the effect of the oxides/carbides on phase transformations. It still remains to distinguish between the various dispersoids present, particularly those of differing morphologies.

## REFERENCES


1. S.J. Savage and F.H. Froes, J. of Metals, Vol. 36, 4, p.20, 1984.
2. A. Lawley, J. of Metals, Vol. 38, 8, p.15, 1986.
3. W.M. Griffith, R.E. Sanders, Jr., and G.J. Hildeman, in High Strength Powder Metallurgy Aluminum Alloys, Edited by: M.J. Koczak and G.J. Hildeman, the Metallurgical Society of AIME, Warrendale, PA., p.209, 1982.
4. N.J. Grant, ibid., reference number 3, p.3.
5. Rapidly Solidified Powder Aluminum Alloys, Edited by M.E. Fine and E.A. Starke, Jr., ASTM Special Technical Publication 890, Am. Soc. for Testing and Materials, Philadelphia, PA., 1986.
6. High Strength Powder Metallurgy Aluminum Alloys II, Edited by: G.J. Hildeman and M.J. Koczak, The Metallurgical Society, Inc., Warrendale, PA., 1986.
7. D.L. Yaney, J.C. Gibeling and W.D. Nix, in Strength of Metals and Alloys, Edited by: H.J. McQueen, J.P. Bailon, J.I. Dickson, J.J. Jonas and M.G. Akben, Pergamon Press, Oxford, P.887, 1986.
8. Y. Kim and W.M. Griffith, ibid., reference number 5, p.485.
9. D.L. Yaney and W.D. Nix, Met. Trans., Vol. 18A, p.893, 1987.
10. L. Angers, M.E. Fine and J.R. Weertman, Met. Trans., Vol. 18A, p.555, 1987.
11. Aluminum Alloys: Their Physical and Mechanical Properties, Edited by: E.A. Starke, Jr., and T.H. Sanders, Jr., The Chameleon Press, London, 1986.
12. Y. Kim, W.M. Griffith and F.H. Froes, J. of Metals, Vol. 32, 8, p 27, 1985.
13. M.K. Premkumar, A. Lawley and M.J. Koczak, in Modern Developments in Powder Metallurgy, Edited by: E.N. Aqua and C.I. Whitman, Metal Powder Industries Federation, Princeton, NJ., U.S.A., Vol. 16, p.467, 1985.
14. M.K. Premkumar, "A Fundamental Study of P.M Processed Elevated Temperature Aluminum Alloys", Ph.D. Dissertation, Department of Materials Engineering, Drexel University, Philadelphia, PA, 1985.
15. M.K. Premkumar, M.J. Koczak and A. Lawley, ibid., reference number 6, p 265
16. J.S. Benjamin, Met. Trans., Vol. 1A, p.2943, 1970.

17. J.S. Benjamin, Scientific American, Vol. 234, 5, p.40, 1976.
18. J.S. Benjamin and M.J. Bomford, Met. Trans., Vol. 8A, p.1301, 1977.
19. G. Jangg, F. Kutner and G. Korb, Powder Metall. Int., Vol. 9, p.24, 1977.
20. P.S. Gilman and W.D. Nix, Met. Trans., Vol. 12A, p.813, 1981.
21. R.F. Singer, W.C. Oliver and W.D. Nix, Met. Trans., Vol. 11A., pp.1895, 1980.
22. S.S. Ezz, M.J. Koczak, A. Lawley and M.K. Premkumar, ibid., reference number 6, p.287.
23. S.S. Ezz, A. Lawley, and M.J. Koczak, ibid., reference number 11, p.1013.
24. R.E. Swanson and Y. Kim, ibid., reference number 11, p. 217.
25. B. Kad and B.F. Oliver, ibid. reference number 11, p. 1039.

**Table I: Steady State Creep Rate**

| | | non-MA | MA |
|---|---|---|---|
| 350°C | 103 MPa | $4.1 \times 10^{-7} s^{-1}$ | $8.3 \times 10^{-10} s^{-1}$ |
| 380°C | 83 MPa | $2.6 \times 10^{-7} s^{-1}$ | $1.6 \times 10^{-9} s^{-1}$ |
| 380°C | 103 MPa | $4.9 \times 10^{-5} s^{-1}$ | $1.4 \times 10^{-9} s^{-1}$ |

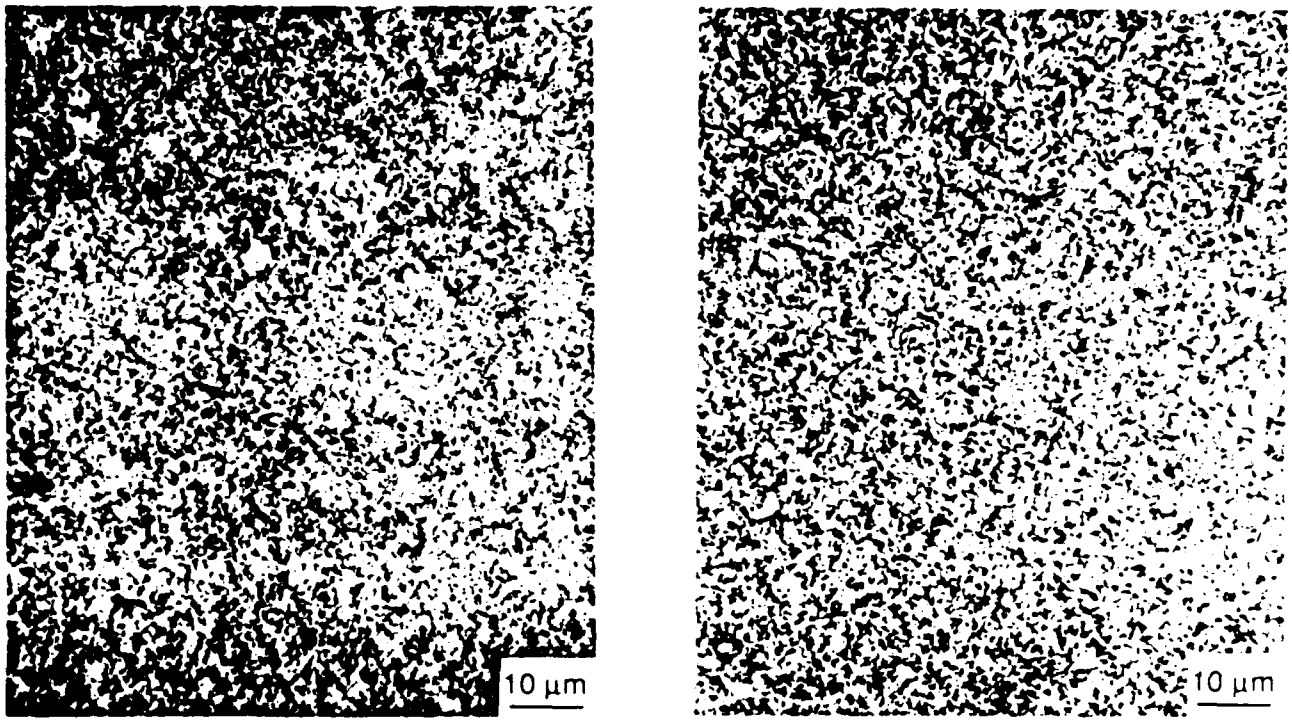


(a) (b)

Figure 1 As-extruded Al-Fe-Ce (a) non-MA, (b) MA.

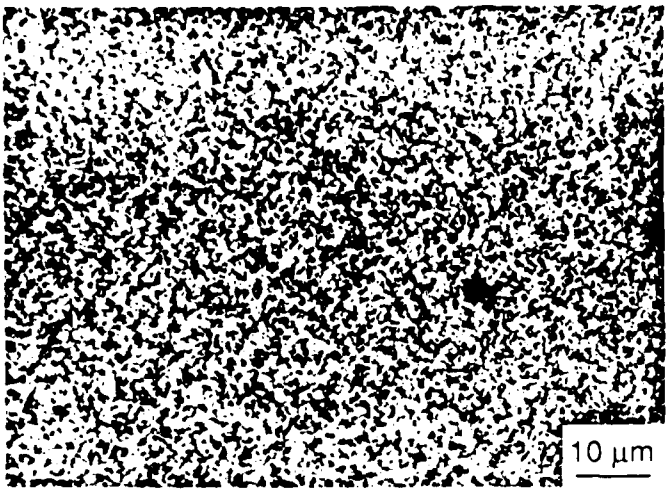


(a)

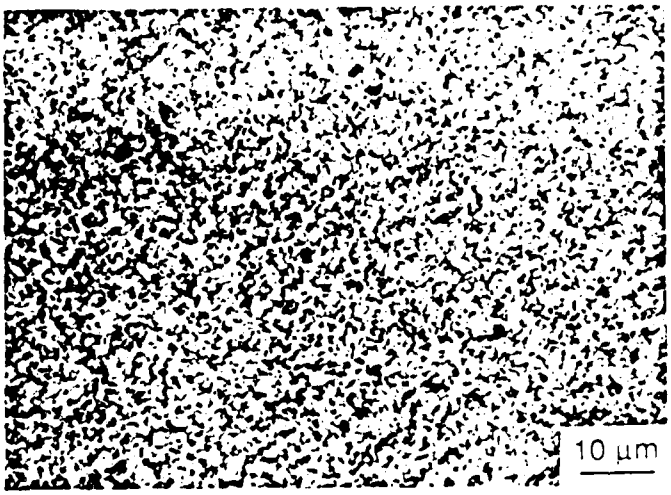


(b)

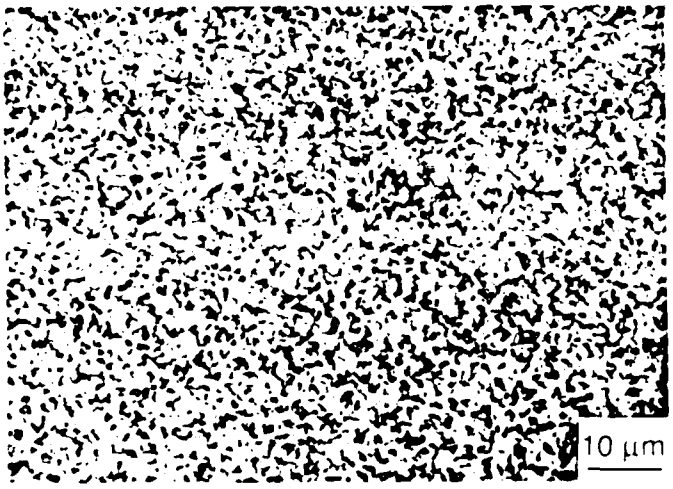


(c)

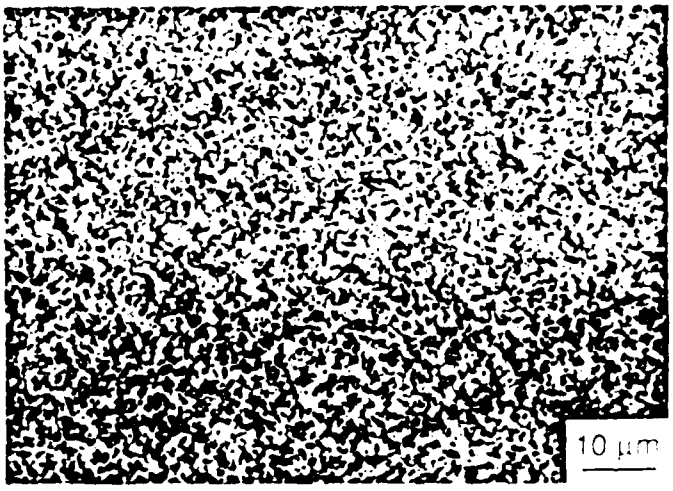


(d)

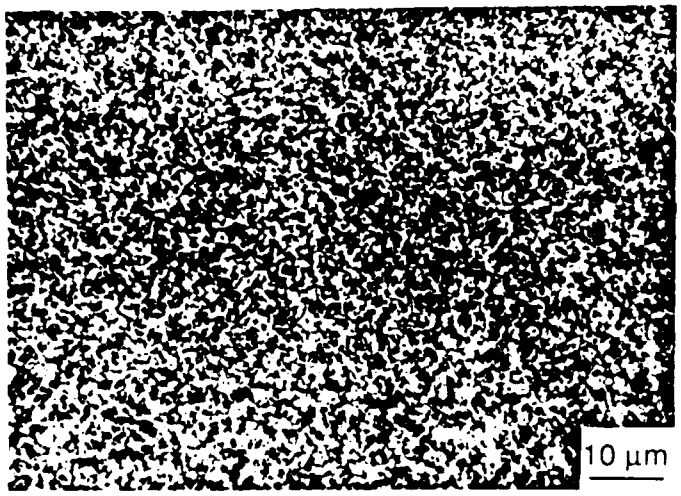


(a)

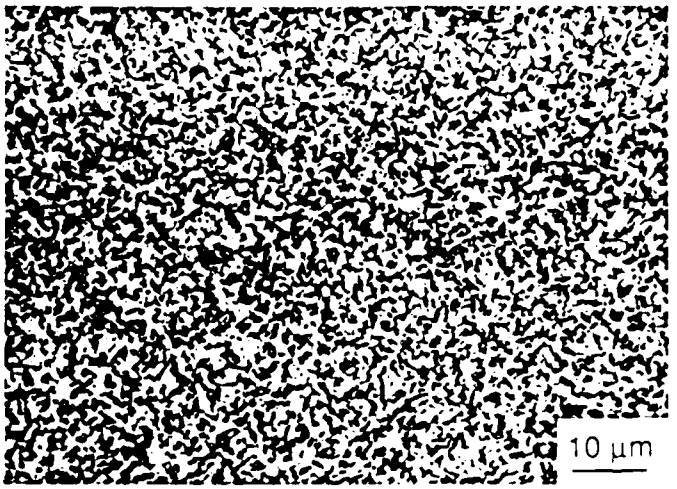


(b)

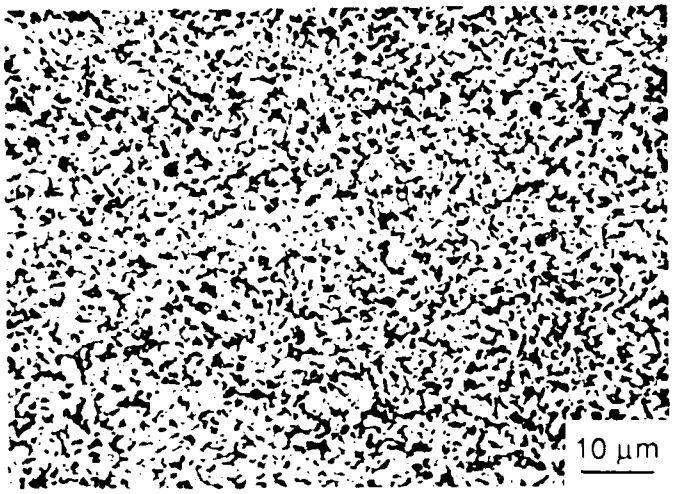


(c)

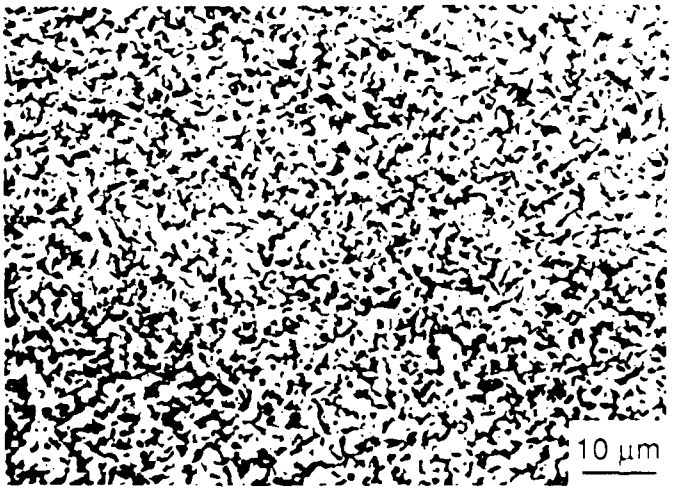


(d)

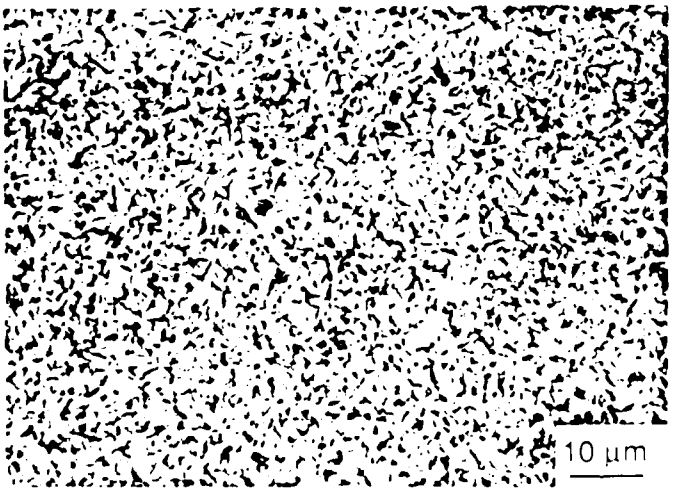


(e)

Figure 3. MA (a) 420 C 1hr, (b) 450 C 8hr, (c) 450 C 50 hr, (d) 450 C 288 hr, (e) 603 C 1hr

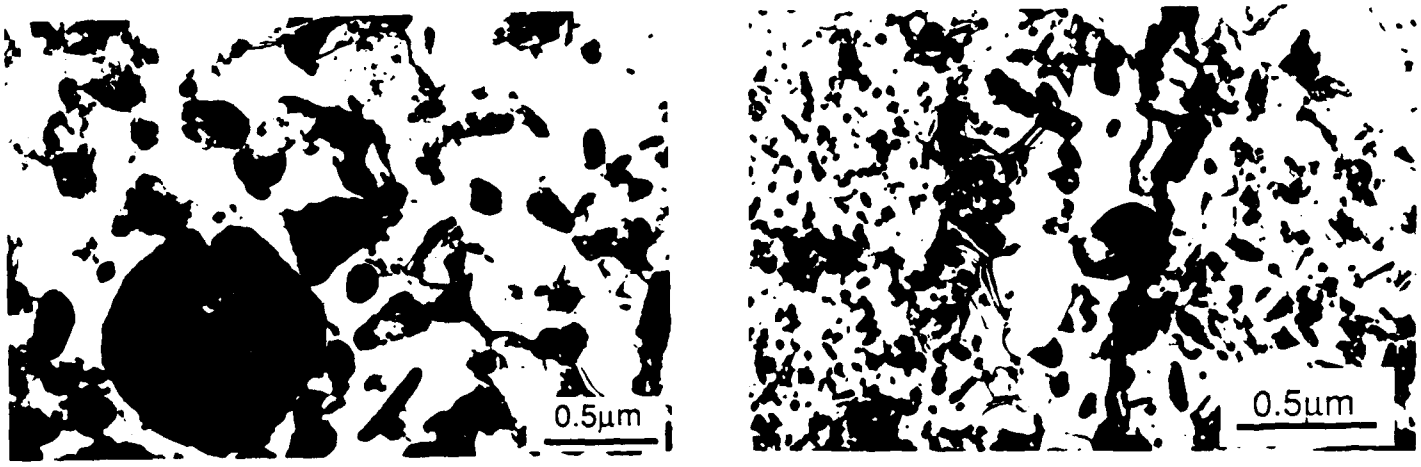


(a)

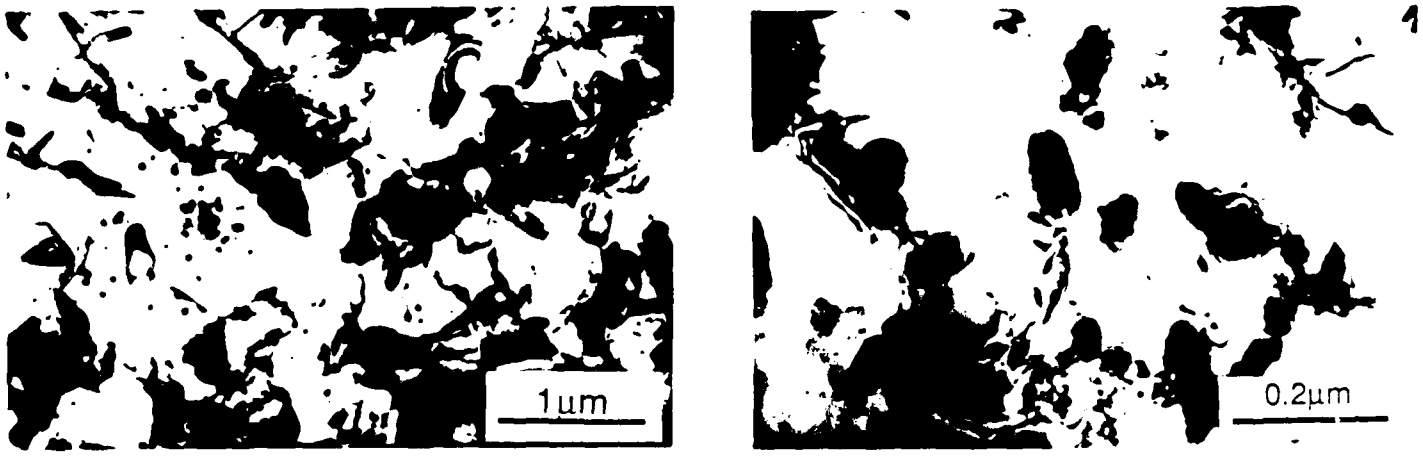


(b)

Figure 4: As extruded Al-Fe-Ce (a) non-MA, (b) MA.

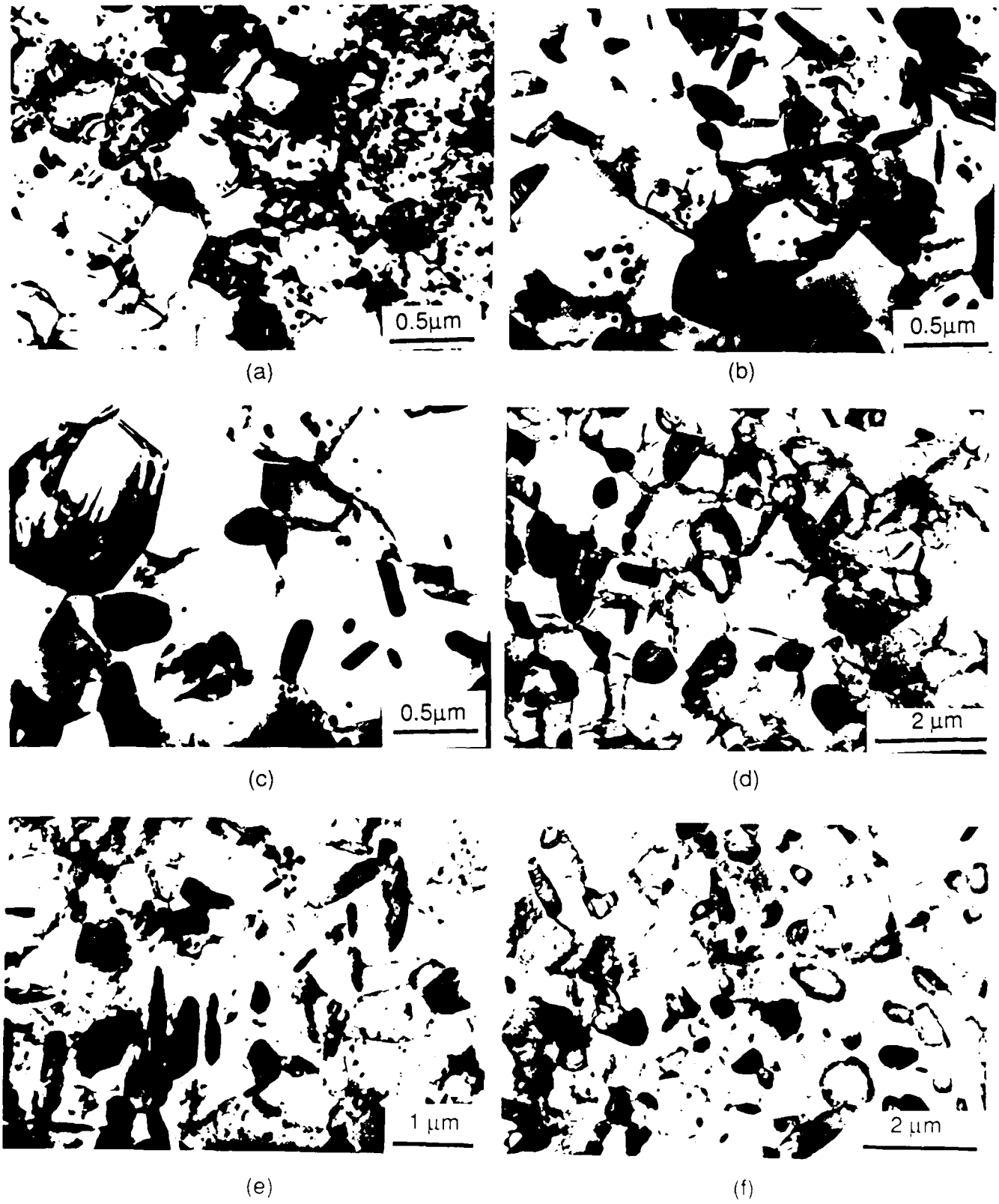


Figure 5: Non MA (a) 420 C/1hr., (b) 450 C 8hr., (c) and (d) 450 C 288 hr., (e) and (f) 603 C/1hr.

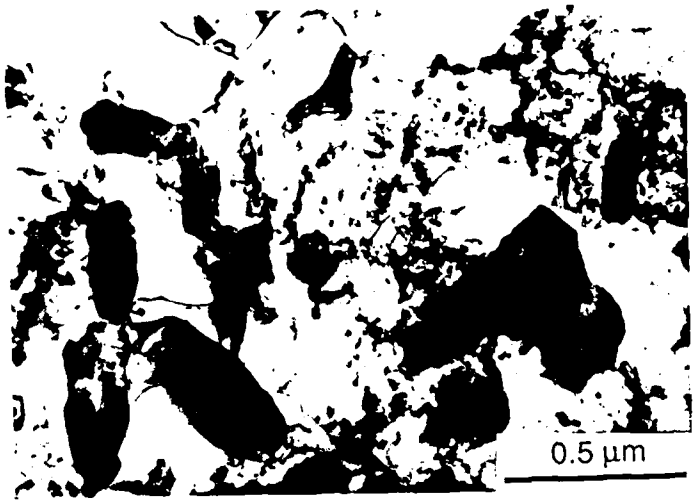


(a)

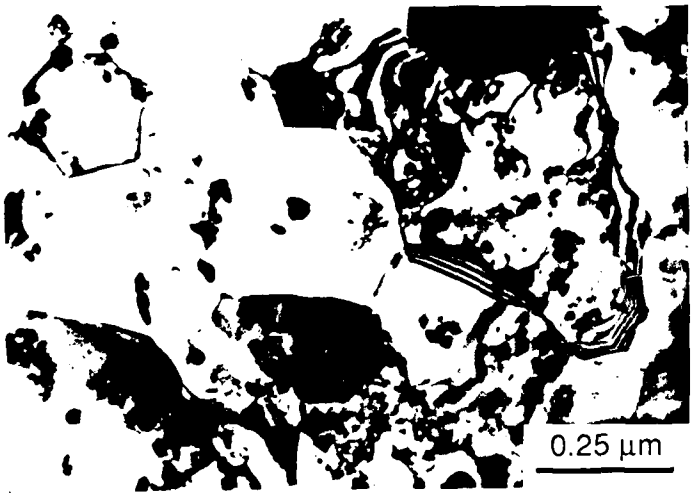


(b)

Figure 6: MA (a) 533°C/1.5 hr., (b) 610°C/1 hr.

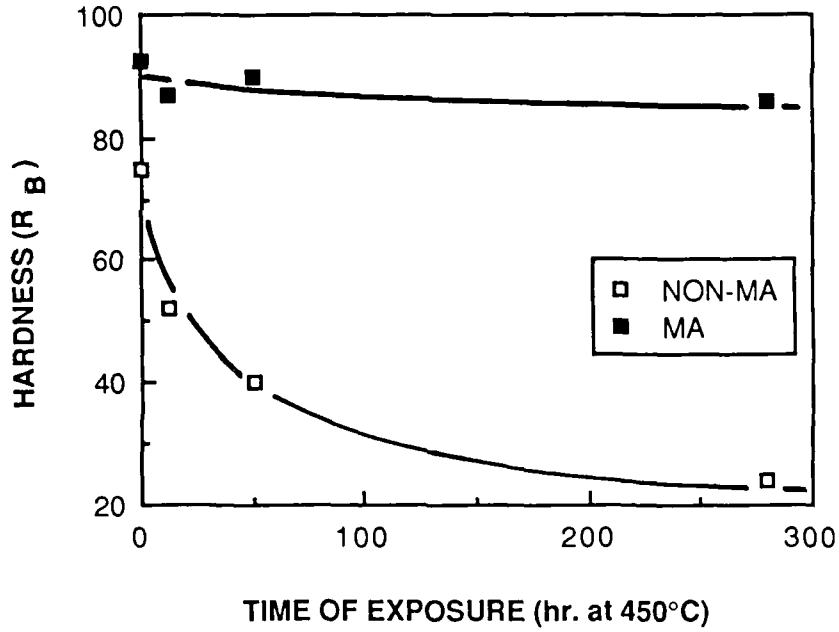


Figure 7: Room temperature hardness following elevated temperature exposure (isothermal).

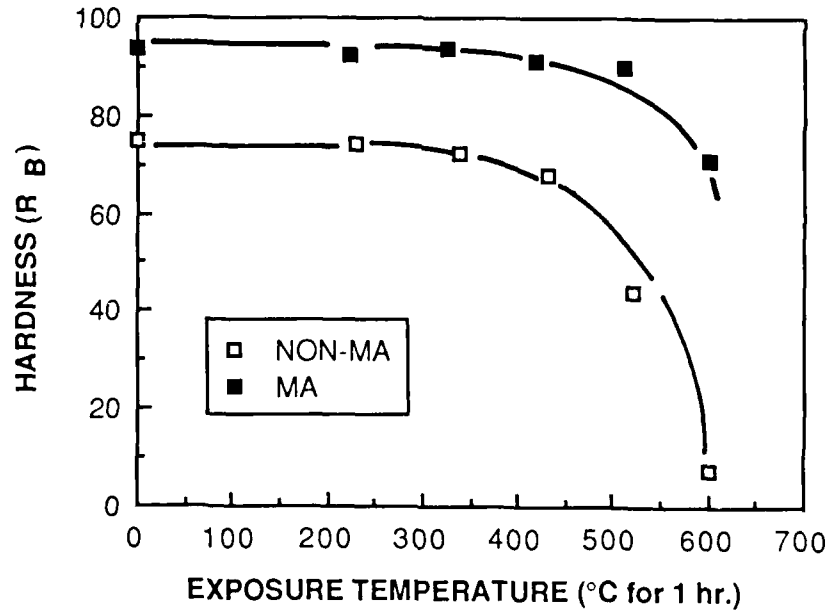


Figure 8: Room temperature hardness following elevated temperature exposure (isochronal).

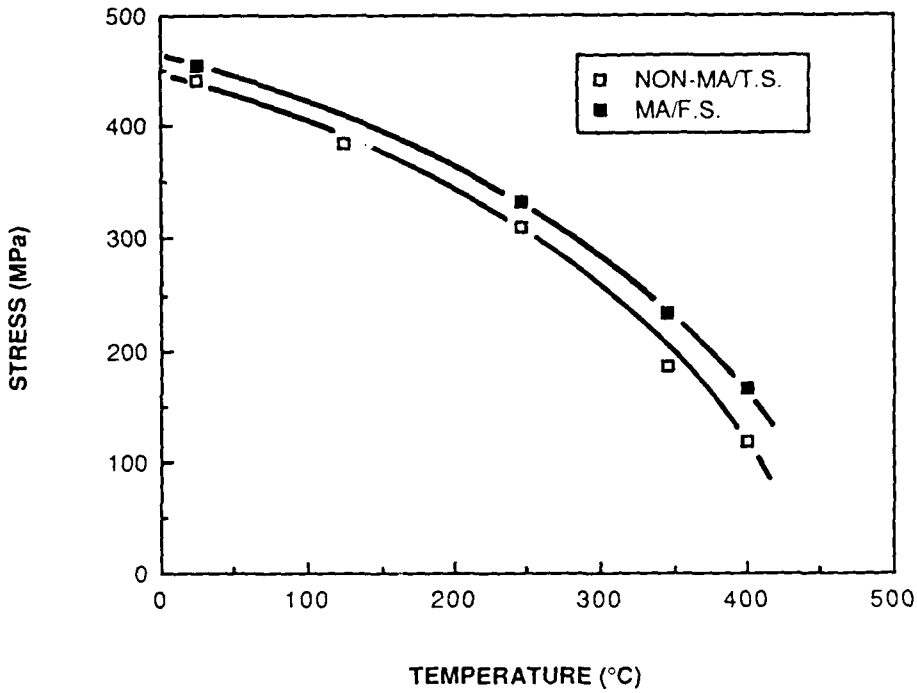


Figure 9: Temperature dependence of strength; non-MA and MA Al-Fe-Ce.

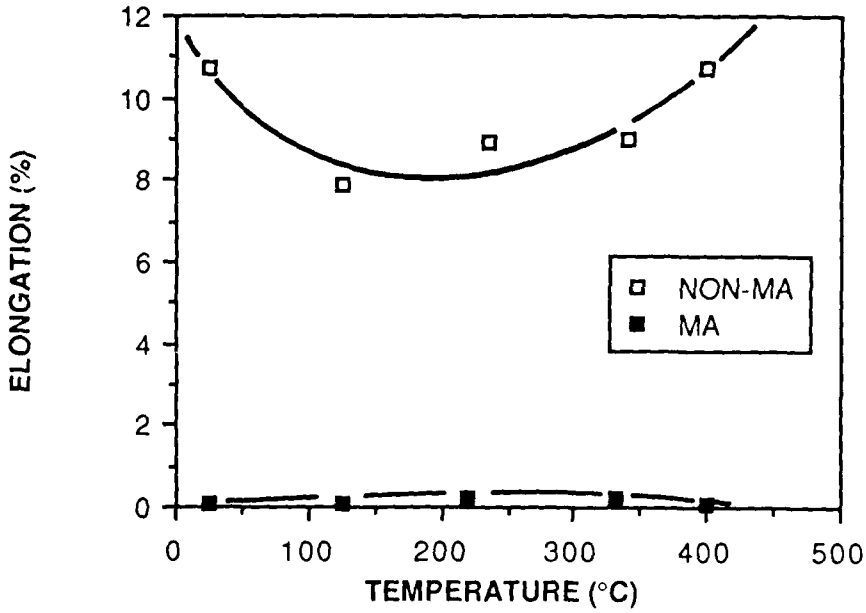


Figure10: Temperature dependence of ductility; non-MA and MA Al-Fe-Ce.

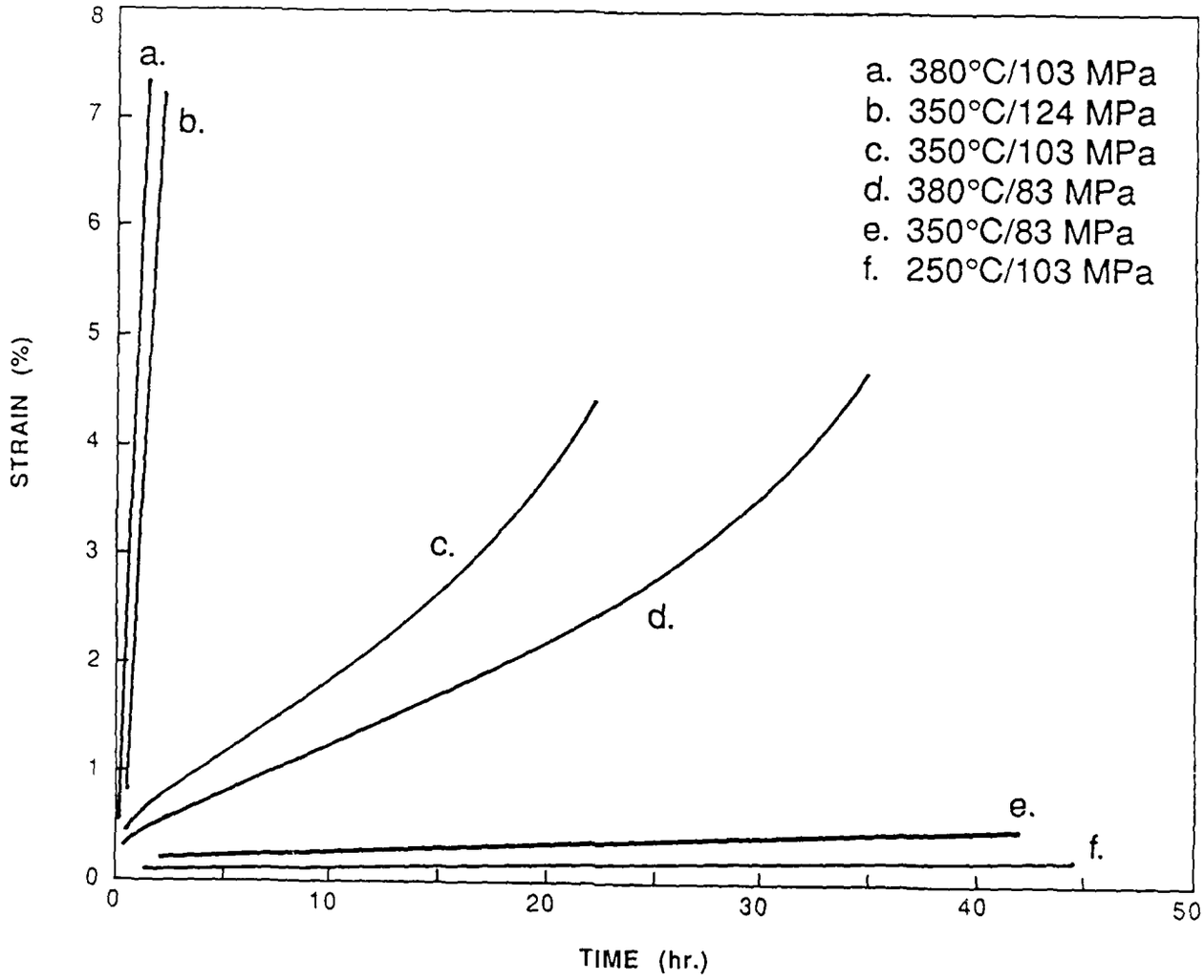


Figure 11. Creep curves; non-MA Al-Fe-Ce.

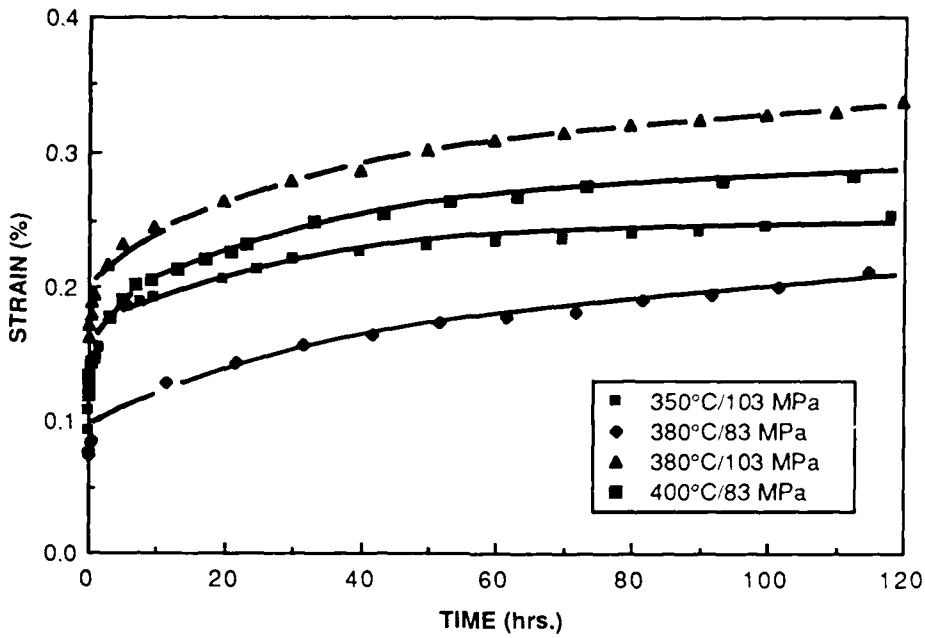


Figure 12: Creep curves; MA Al-Fe-Ce.

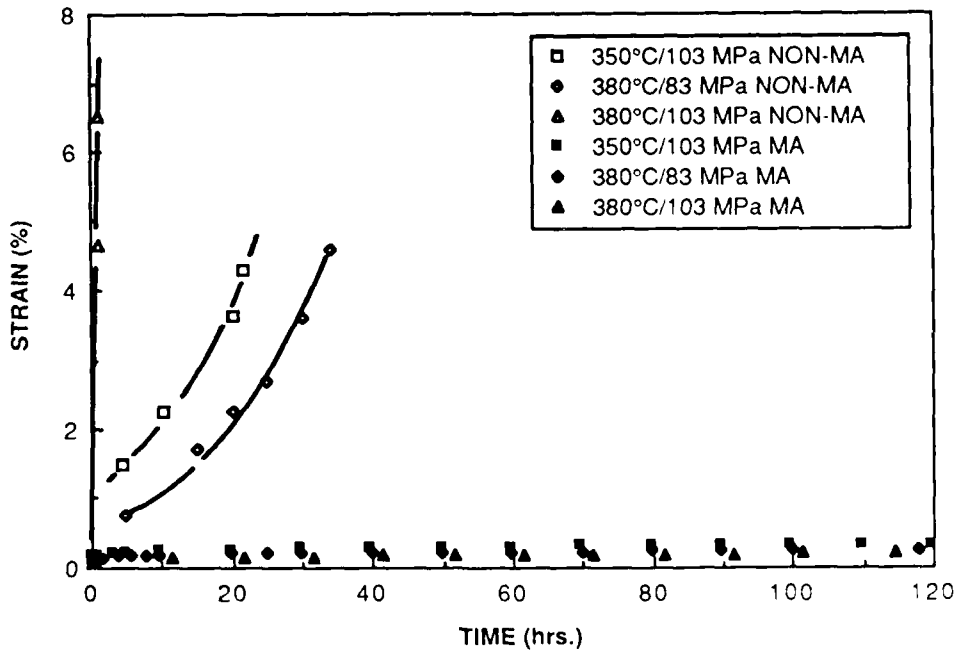


Figure 13: Comparison of creep curves for non-MA and MA Al-Fe-Ce.

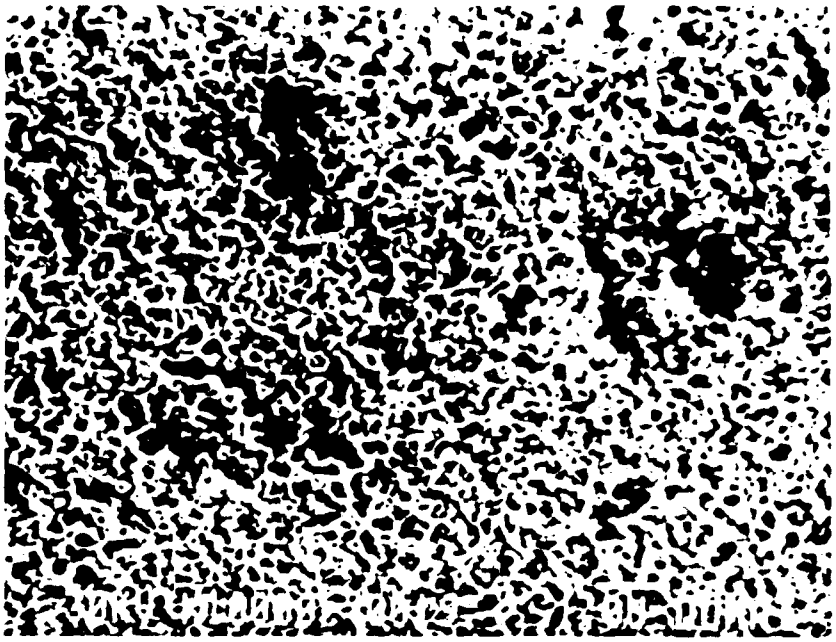

(a)

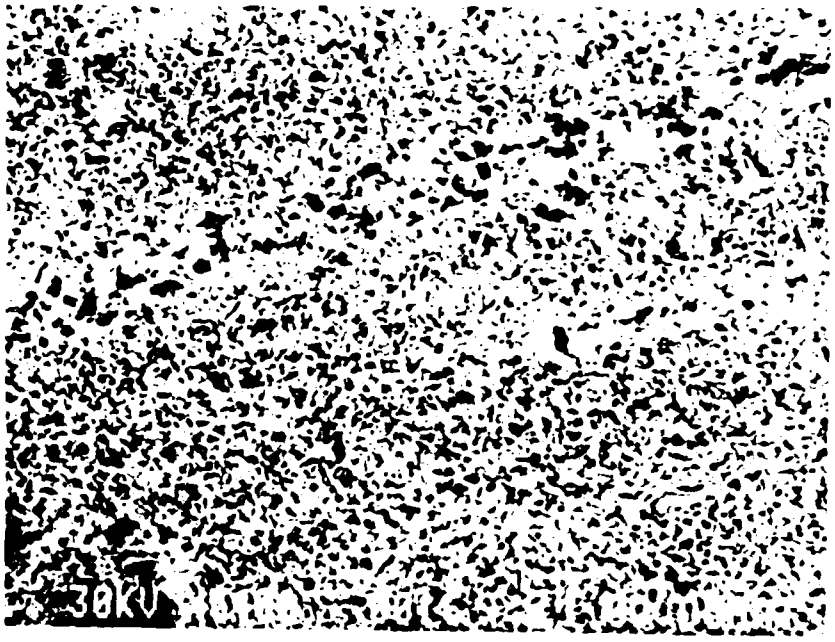


(b)

Figure 14: Microstructure beneath fracture surface; tensile deformation at 400 C (a) non-MA, (b) MA.

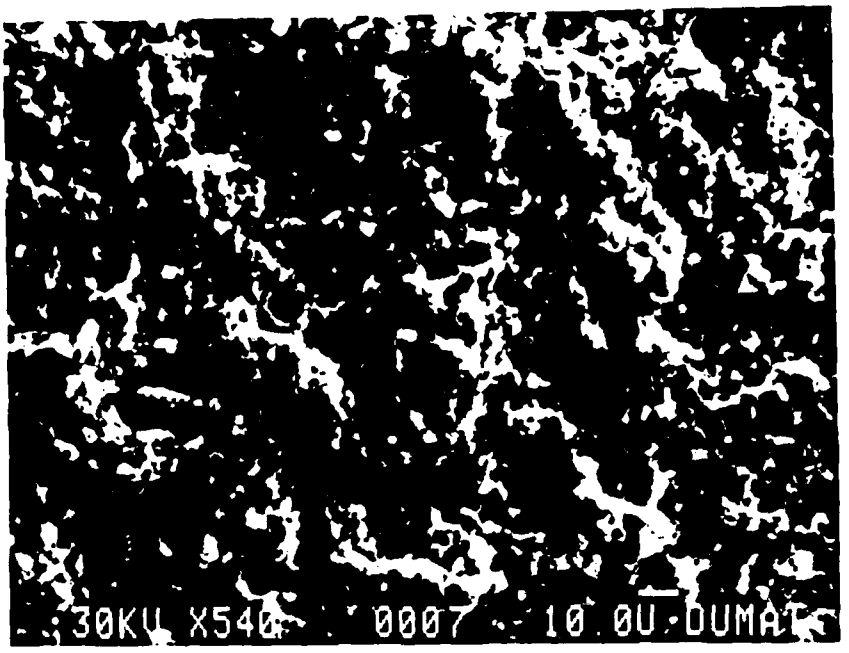


(a)

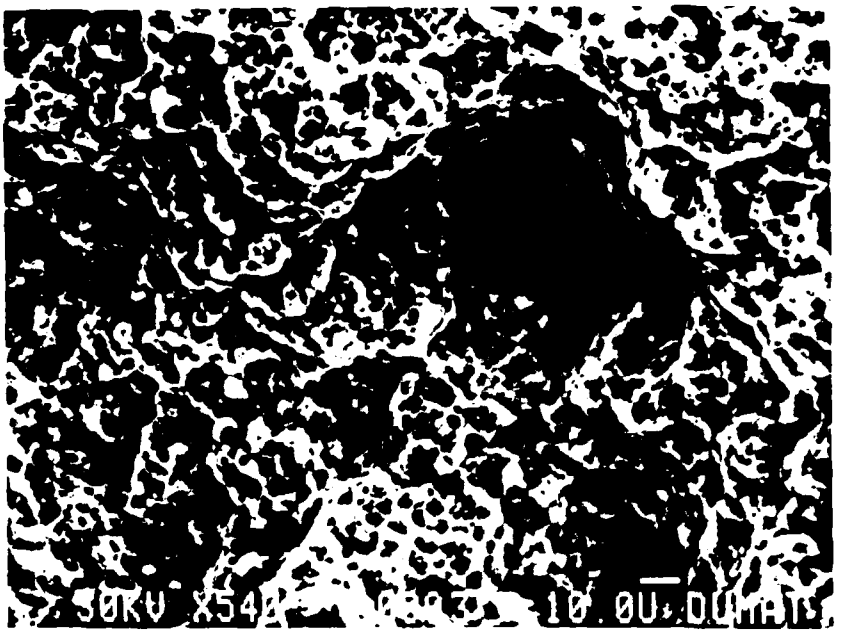


(b)

Figure 15: Tensile fracture surfaces; non-MA Al-Fe-Ce (a) room temperature, (b) 340°C.

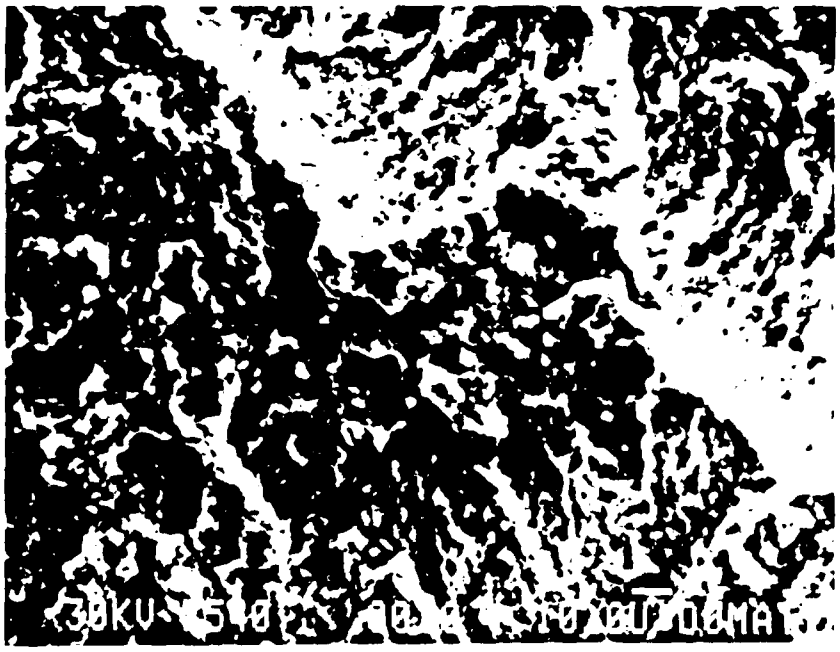


(a)

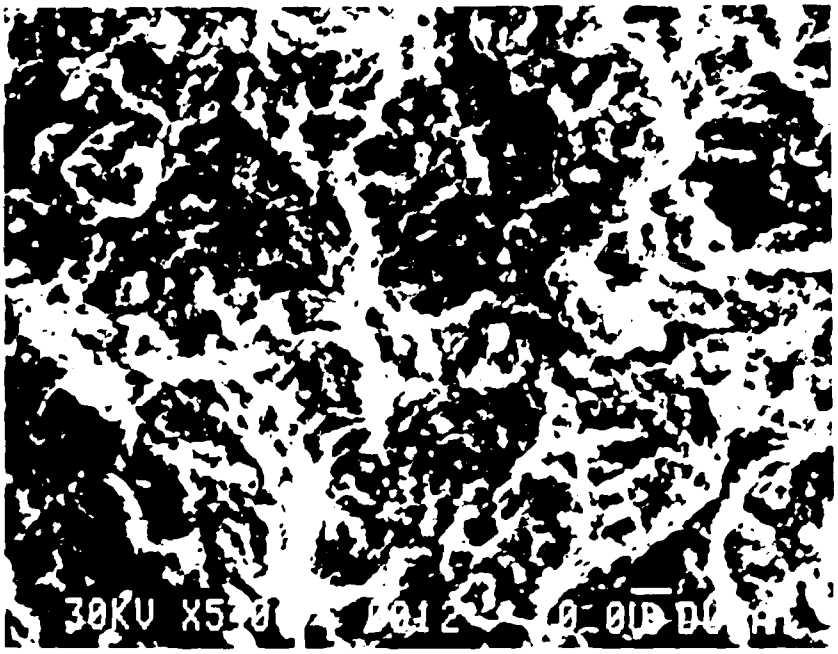


(b)

Figure 16: Tensile fracture surfaces; MA Al-Fe-Ce (a) room temperature, (b) 340 C.

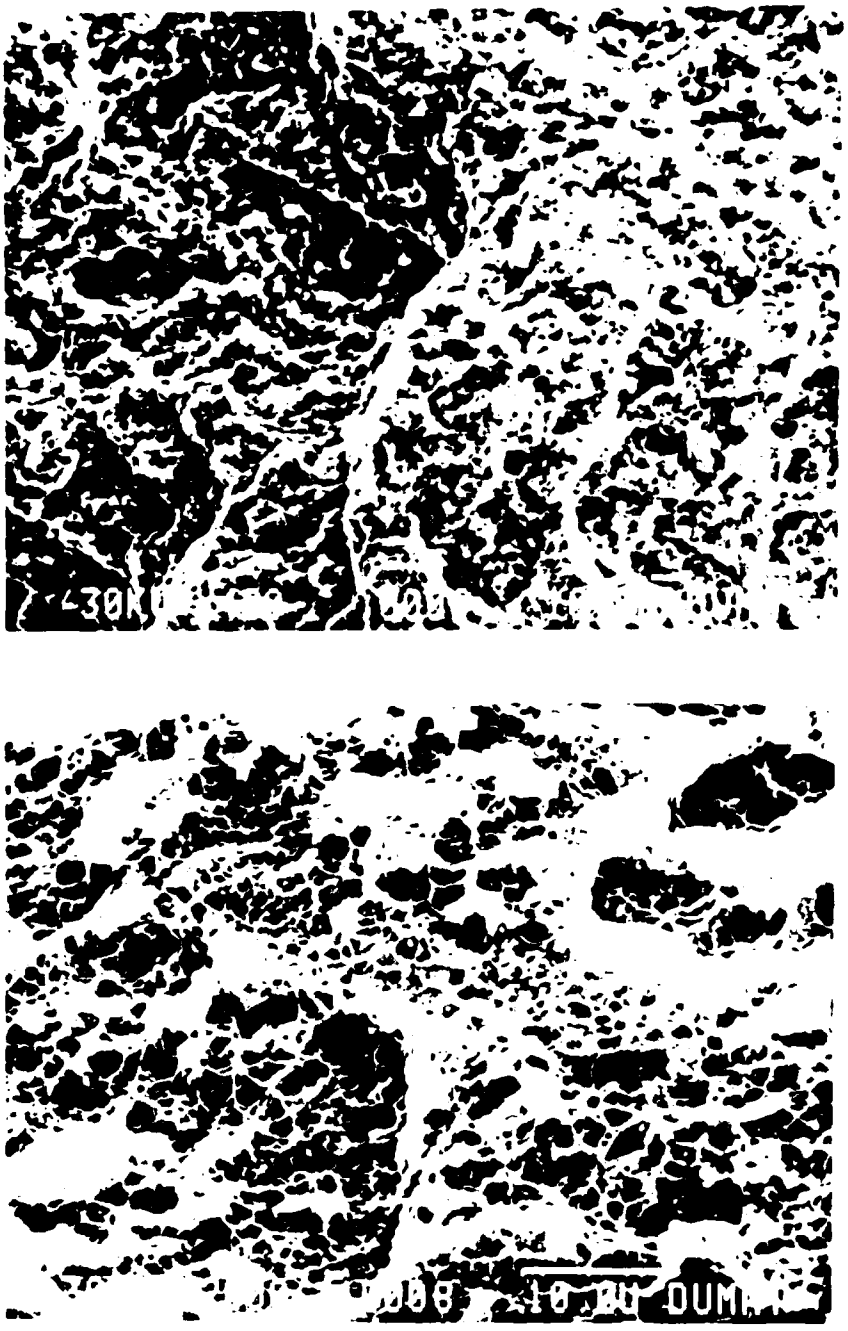

Figure 17: Creep fracture surface; non MA Al-Fe-Ce 350 C 103 MPa

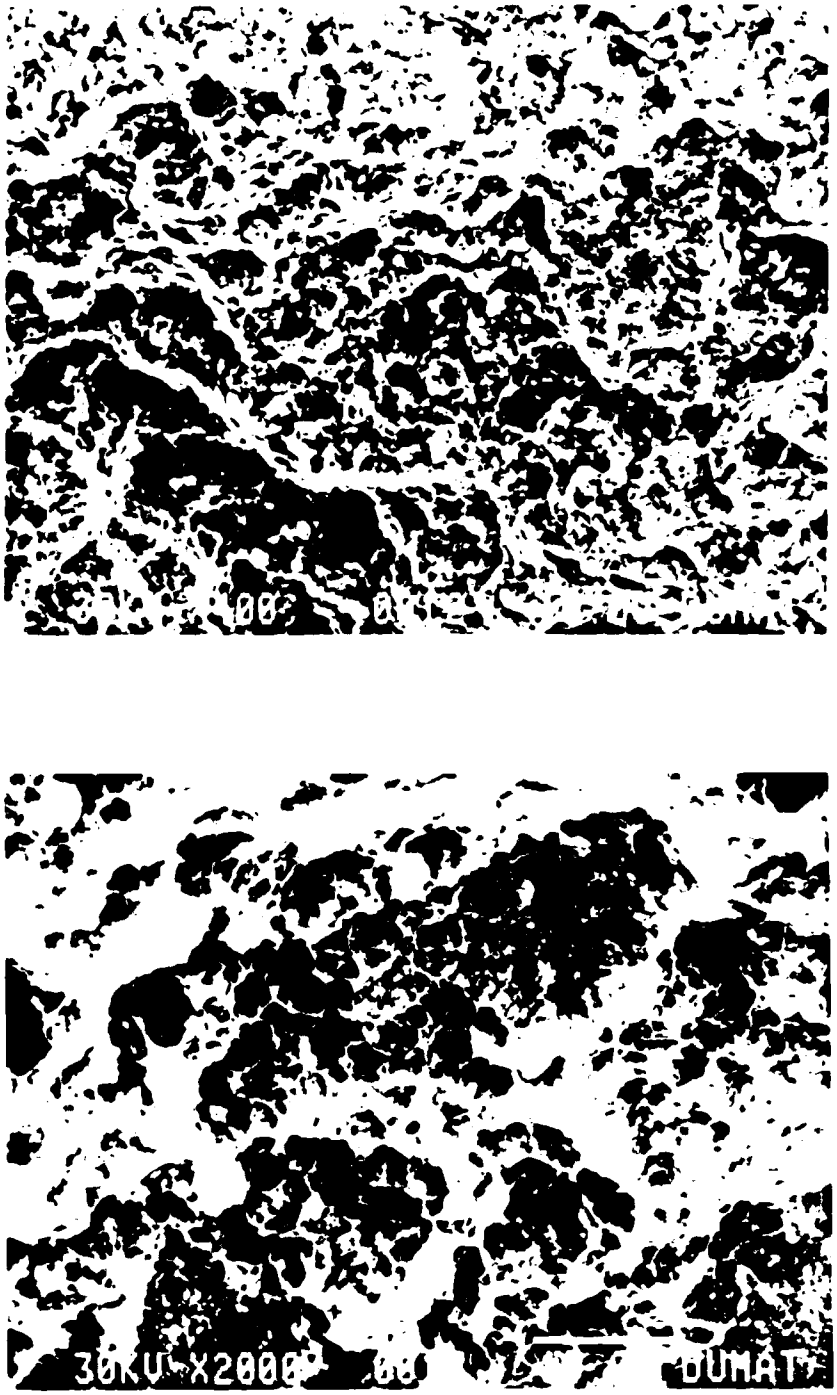


Figure 18 Creep fracture surface, non-MA Al-Fe-Ce 350 C 124 MPa

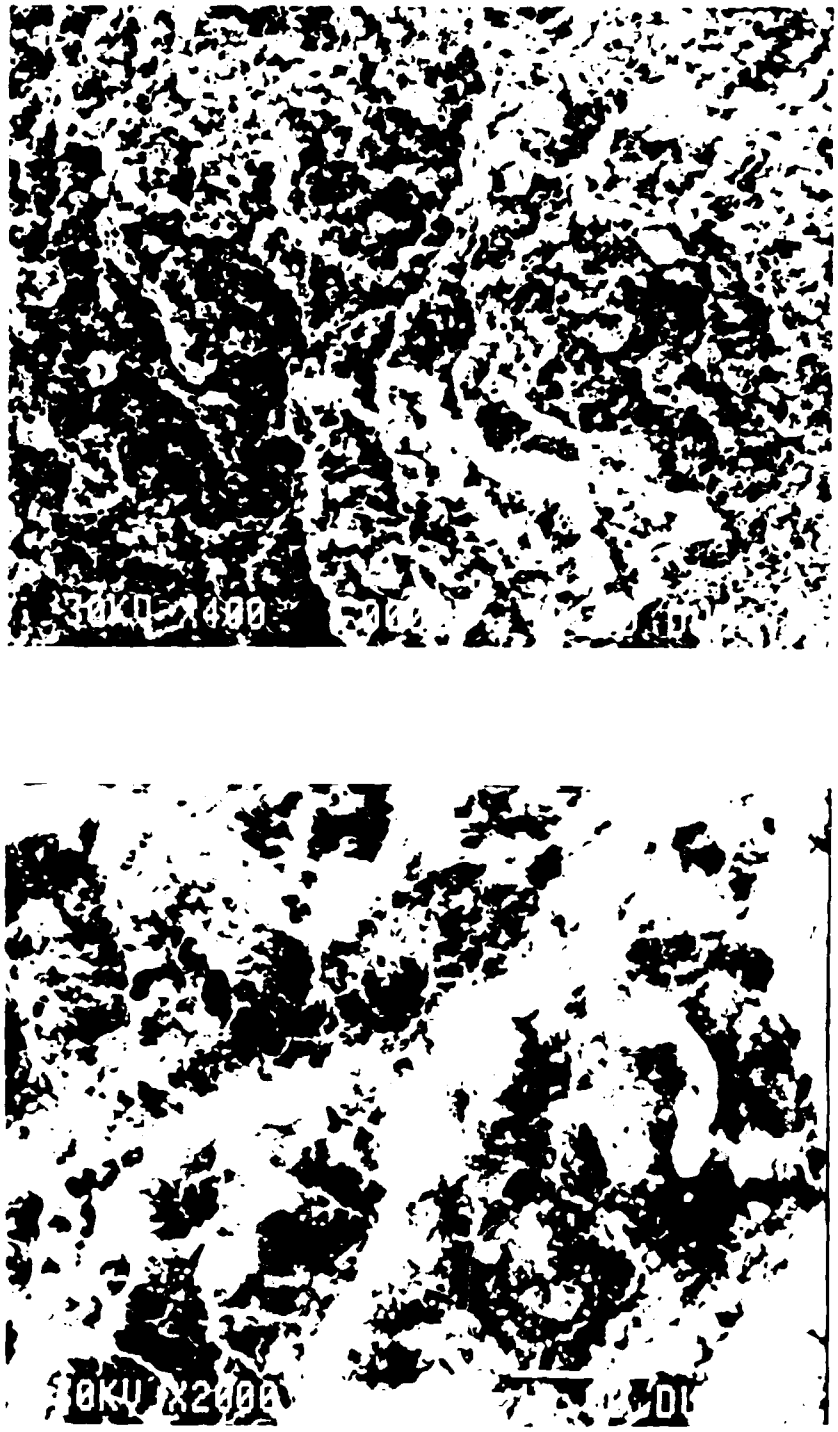


Figure 19 Creep fracture surface; non-MA Al-Fe-Ce 380°C/83 MPa.

## PUBLICATIONS AND DISSERTATIONS

The following publications reflect work performed as a result of this program:


E.Y. Gutmanas and A. Lawley, "Cold Sintering - A New Powder Consolidation Process" in Progress in Powder Metallurgy, Editors: H.S. Nayar, S.M. Kaufman and K.E. Meiners, Metal Powder Industries Federation, Princeton, N.J. Vol. 39, p. 653 (1984).

E.Y. Gutmanas, M.K. Premkumar, and A. Lawley, "Microstructure and Mechanical Properties of Cold Sintered P/M Aluminum Alloys", Progress in Powder Metallurgy, Editors: H.S. Nayar, S.M. Kaufman and K.E. Meiners, Metal Powder Industries Federation, Princeton, N.J., Vol. 39, p. 669 (1984).

M.K. Premkumar, A. Lawley and M.J. Koczak, "Dispersion Strengthened Aluminum Alloys for Elevated Temperature Applications", in Powder Metallurgy in Defense Technology, Editors: C.L. Freeby and W.J. Ullrich, Metal Powder Industries Federation, Princeton, N.J., Vol. 6, p. 153 (1985).

M.K. Premkumar, A. Lawley and M.J. Koczak, "Elevated Temperature Properties of a Powder-processed Al-Ni-Fe Alloy" in Modern Developments in Powder Metallurgy, Editors: C.I. Whitman and E.N. Aqua, Metal Powder Industries Federation, Princeton, N.J., Vol. 16, p. 467 (1985).

E.Y. Gutmanas, O. Botshtein and A. Lawley, "Thermal Stability and Mechanical Behavior of Cold Sintered P/M Aluminum Alloys", in Modern Developments in Powder Metallurgy, Editors: C.I. Whitman and E.N. Aqua, Metal Powder Industries Federation, Princeton, N.J. Vol. 15, p. 761 (1985).

O. Botshtein, E.Y. Gutmanas and A. Lawley, "High Pressure Consolidation of a Dispersion Strengthened Aluminum Alloy", in Progress in Powder Metallurgy, Editors: H.L. Sanderow, W.L. Giebelhausen and K.M. Kulkarni, Metal Powder Industries Federation, Princeton, N.J., Vol. 41, p. 123 (1986).

M.K. Premkumar, M.J. Koczak and A. Lawley, "Elevated Temperature Mechanical Behavior of P/M Dispersion Strengthened Al-Fe-Ni Alloys", in High Strength Powder Metallurgy Aluminum Alloys II, Editors: G.J. Hildeman and M.J. Koczak, The Metallurgical Soc. Inc., Warrendale, P.A., p. 265 (1986).

S.S. Ezz, M.J. Koczak, A. Lawley and M.K. Premkumar, "Strength and Microstructural Stability of Mechanically Alloyed Al-Fe-Ni", in High Strength Powder Metallurgy Aluminum Alloys II, Editors: G.J. Hildeman and M.J. Koczak, The Metallurgical Soc.

Inc., Warrendale, P.A., p. 287 (1986).

S.S. Ezz, A. Lawley and M.J. Koczak, "Dispersion Strengthened Al-Fe-Ni: A Dual Rapid Solidification - Mechanical Alloying Approach", in Aluminum Alloys: Their Physical and Mechanical Properties, Editors: E.A. Starke, Jr. and T.H. Sanders, Jr., The Chameleon Press, Ltd., London, Vol. 11, p. 1013 (1986).

**DOCTORAL DISSERTATION**

M.K. Premkumar, "A Fundamental Study of P/M Processed Elevated Temperature Aluminum Alloys", Drexel University, Department of Materials Engineering, Philadelphia, P.A., June 1985.

END

11-87

DTIC